Tunneling in artificial Al_2O_3 tunnel barriers and Al_2O_3-metal multilayers

J. B. Barner and S. T. Ruggiero
Department of Physics, University of Notre Dame, Notre Dame, Indiana 46556
(Received 21 July 1988)

We report on the material and electron-tunneling properties of thin Al_2O_3 films deposited onto room-temperature substrates by rf magnetron sputtering of a pressed aluminum oxide target in a pure argon atmosphere. X-ray photoelectron spectroscopy shows the films to be composed of $>99\%$ Al_2O_3. The electrical properties have been investigated by tunneling in junctions of the form: Cu/Al_2O_3/counterelectrodes with counterelectrodes of Cu, Pb, and Pb-Bi. The Cu/Al_2O_3 bilayers were deposited *in situ* with Al_2O_3 thicknesses ranging from 8 to 20 Å. These junctions have been found to exhibit excellent tunneling characteristics including low zero-bias conduction (typically below 1% at 4.2 K) and large effective barrier heights (typically above 1 eV). We have observed full, clean superconducting gap structure, and strong, clear phonon structure for junctions with Pb-Bi counterelectrodes. The expected exponential rise of junction resistance with increasing barrier thickness was observed, giving an average barrier height of 1.65 eV and an effective tunneling length of 0.82 Å. We observe a steplike increase in junction yield as barrier thickness exceeds 12–15 Å, the dependence of which has been successfully modeled as a statistical buildup of barrier molecules on the base-electrode surface. We have also investigated the tunneling characteristics of metal/Al_2O_3/intermediate metal/Al_2O_3/metal multilayer junctions wherein the properties of the intermediate metal films can be studied and have provided a confirmation of single-electron tunneling effects.

I. INTRODUCTION

Electron tunneling has long been used to investigate the properties of thin-film materials and has served as the basis of a wide range of devices. Until relatively recently, the successful preparation of tunnel junctions meant the use of native-oxide growth to form the tunnel barrier. Unfortunately, native-oxide formation can be unreliable, difficult to achieve on a given material of interest, or otherwise problematical. Recently, however, many of these problems have been overcome by the use of so-called artificial tunnel barriers, which can enhance or completely substitute for native-oxide formation and thereby permit tunneling into virtually any material of interest.

In the present work, we discuss our results on the preparation of artificial barriers using the direct deposition of Al_2O_3 onto Cu base electrodes. This is similar in nature to that of other groups using MgO (Refs. 1–4) and related materials[2,5]—work stemming from the preparation of barriers on NbN. The motivation for our studies was twofold: (1) to create a flexible technique for the preparation of barriers on an arbitrary material and (2) to create more complex metal/barrier/intermediate metal/barrier/metal $\cdots$ ($M/B/M'/B/M\cdots$) systems with which the properties of the intermediate M' layer could be studied. We discuss here principally the first item and have reported results on the second in short papers[6,7] which will be followed by a more comprehensive work.

To briefly review previous work on the subject, we note that there have been a number of successful techniques developed to form artificial barriers over the last ten years. These fall into three distinct classes. The first was originally demonstrated by Beasely and co-workers[8–10] and involves depositing a semiconductor, in this case Si, onto a base-electrode material to form the barrier either by itself or by following up with an oxidation treatment. It was shown that such barriers, although greatly improving junction properties, resulted in low barrier heights in the case of pure Si (Ref. 11) which improved with oxidation.[12] Indeed, it is now clear that post oxidation of artificial barriers—or the use of other techniques to passivate the base electrode prior to barrier deposition—is effective in plugging pinholes in the artificial barrier which can otherwise lead to poor tunneling properties.

Although semiconducting barriers can indeed significantly improve tunneling characteristics, they clearly are not representative of ideal, rectangular quantum-mechanical barriers—in the case of semiconductors with a relatively low height and width. These barriers are likely more complex, containing states within the barrier which effectively lower its height. For example, it has been shown that the tunneling density of states can be substantially altered in systems incorporating oxidized amorphous-Si barriers[13] and that Si on Ni can result in attenuated spin-polarized tunneling peaks,[11] implying scattering within the barrier. Kroger *et al.*,[14] have also demonstrated that junction characteristics can be improved by the hydrogenation of the Si barriers, presumably due to the saturation of dangling Si bonds. In any case, whether the origin be an intrinsically smaller gap and/or states within the gap, a lower barrier is potentially advantageous in that it affords greater control over junction current density, since much thicker barriers are required to achieve a given current density with semiconductors.

The second approach to forming an artificial barrier is

the surface-layer technique, which takes advantage of the fact that a variety of metals do form excellent native-oxide tunnel barriers. The idea is to use a thin layer of such metals to cap the material of interest to prevent its oxidation, and oxidize the surface layer to completion or near completion to form a barrier. Metals such as Al,[15–19] Mg, Y,[19,20] Zr,[21] Ta,[22] and a variety of rare-earth metals[20,23,24] have been successfully used in this manner. Although initially employed principally with niobium, oxidized Al overlayers on NbN have recently found favor in high-current-density applications.[25]

The drawback to the surface-layer technique is the possibility of proximity-induced contributions to the tunneling density of states due to the presence residual capping metal which can be left over after oxidation,[15,22] although a deconvolution of the proximity density of states can be accomplished numerically.[15] It has also been shown that the overlayer metal can in some cases diffuse into and debase the base-electrode material.[19]

The third class of artificial-barrier formation is based on the direct deposition of an insulator known to be a good tunnel barrier. This approach was initially shown successful by Moodera *et al.*,[26] who deposited Al_2O_3 by electron-beam evaporation onto substrates cooled to 77 K, the results of which promised an excellent method of barrier preparation. The most recent work with direct barrier deposition has focused on the rf sputtering of barrier materials. These include MgO,[1–4,27] MgO-CaO,[2] SiO_2,[27] Al_2O_3,[2,27,28] and the metal fluorides.[2] In addition, there have been successful investigations using reactive-ion-beamed, or dc-sputtered metals in the presence of oxygen, nitrogen, and CF_4 to form MgO,[29] AlN,[5] and AlF_x,[30] respectively, as well as the evaporation of various oxides and fluorides.[2,30]

Most of the work in this area has centered around Josephson-junction fabrication with NbN. For this reason MgO is preferred because of its close lattice match with NbN—by virtue of which the preparation of epitaxial NbN/MgO/NbN structures has been demonstrated.[2] Indeed, thick layers of MgO are often used as underlayers in order to nucleate good NbN base-electrode material.[2,31,32]

In our work, we have studied junctions with artificial barriers of sputtered Al_2O_3 in order to determine its overall tunneling properties. The Al_2O_3 films were deposited by the simple method of rf sputtering of a pressed Al_2O_3 target in a pure argon atmosphere onto room-temperature substrates. Junctions of the form Cu/Al_2O_3/counterelectrode were prepared in which Cu/Al_2O_3 bilayers were deposited *in situ* and completed *ex situ* with Cu, Pb, or Pb-Bi counterelectrodes. Cu base-electrodes were used with the assumption that any oxidation of this base electrode would not significantly contribute to the barrier, permitting an exclusive study of the Al_2O_3 films themselves. Measurements of these junctions reveal that the Al_2O_3 films exhibit excellent barrier characteristics. Typical barrier heights exceed 1 eV and junctions show subgap leakage conduction below 1% for good junctions. We discuss the material properties of these Al_2O_3 films and their electrical properties as derived from tunneling measurements. We have also examined the effective barrier parameters, superconducting tunneling properties, yield of junctions, and junction resistance all as a function of barrier thickness. Finally, we present a brief discussion of the successful application of these barriers to the study of metal-barrier multilayer structures.

II. EXPERIMENT

Tunnel junctions prepared for these studies were of the form $Cu/Al_2O_3/C$ with counterelectrodes (C) of Cu, Pb, or Pb–29 wt. % Bi. The Cu and Al_2O_3 depositions were performed in a cryo-pumped, 46-cm-diam, stainless-steel deposition chamber. Used in these experiments are two magnetron-type sputter sources,[33] one of which is driven by a dc and the other by an rf power supply. Each source holds a two-inch-diameter target. The pressed aluminum oxide (99.99% Al_2O_3) (Ref. 34) target used for these studies contained various oxide impurities, the most abundant of which were SiO_2(0.018%), CaO($<0.008\%$), Na_2O($<0.008\%$), and Ga_2O_2(0.007%). During these studies, base pressures typically ranged from $(1.1–1.7)\times10^{-7}$ Torr as read on a Perkin Elmer extended-range ion gauge. These pressures were reached within 6–12 h. Shown in Fig. 1 is a typical mass spectrum taken at 1.2×10^{-7} Torr. Present, in order of relative abundance and indicated in Fig. 1, are the residual gases N_2, H_2O, and O_2.

The following sequence was followed for a normal sample run. After pump-down, research-grade (99.996%) argon was admitted to the chamber at a rate of 100 cm^3/min. The argon pressure in the chamber was fixed at 5 mTorr by adjusting a mechanical variable orifice placed in front of the cryopump. The argon was allowed to flow for 5–15 min prior to operation of the sputter sources in order to assure a clean background environment. The dc (Cu) and rf (Al_2O_3) sources were then ignit-

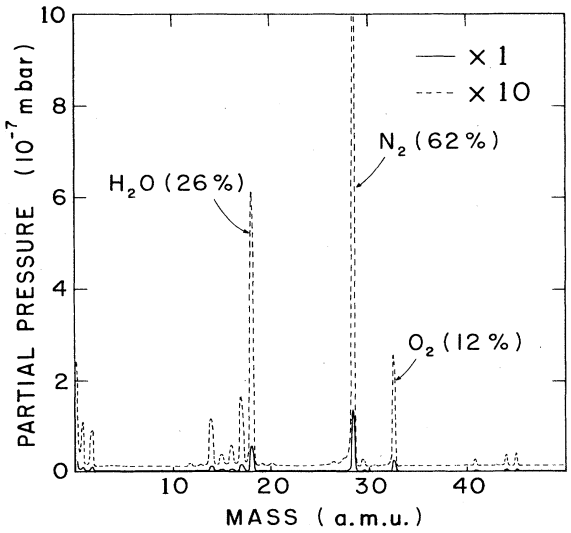

FIG. 1. Typical residual-gas spectrum for our sputter-deposition system at 10^{-7} Torr. Indicated are the major residual gases in percentages of the total background pressure.

ed and predeposition sputtering was performed for typically 5, but no less than 2 min. During this period the rf supply was set for 200 W of forward power, normally resulting in 8–10 W of reflected power, and a Cu deposition rate was held at 10 Å/sec as measured by a quartz-crystal monitor. After this predeposition cleaning period, the rf power was increased to 300 W forward, resulting in typically 12–17 W of reflected power. The resulting Al_2O_3 deposition rate was roughly 1 Å/sec, having been previously established by measuring the thickness of a nominally 300-Å-thick film with a Sloan profilometer. Determination of the Al_2O_3 deposition rate in this manner was repeated occasionally to insure accurate film thicknesses throughout the life of the target. This method of determining the rate was necessary due to the fact that the crystal monitor does not detect either a rate for or an accumulation of any aluminum oxide, for reasons which are not fully understood.

Sample substrates used were 5.08-cm-diam, single-crystal, [111], *p*-type (boron doped) Si wafers with a room-temperature resistivity of 1–5 Ω cm. In order to form junctions, mechanical masks were used to define film geometries. Approximately 30 individual tunnel junctions were ultimately created on each wafer. After the previously described predeposition procedure had been completed, the substrate received a 500 Å-thick Cu base-electrode film through a slotted mask with 0.254-cm-wide grooves. It was then rotated above the Al_2O_3 source (within one second) to deposit the barrier. Separate runs were made during which Al_2O_3 thicknesses of 8, 10, 12, 15, and 20 Å were deposited. While the sample was above either source, it was oscillated back and forth at about 2 Hz to enhance film uniformity. After depositing the Cu/Al_2O_3 bilayers, the sources were turned off. We then (1) allowed the argon to continue to flow for 15 to 30 min, (2) pumped the chamber down to normal base pressures, and (3) allowed the substrate and sources to cool for one to two hours.

After this, the sample was removed from the sputter-deposition chamber and transferred to a standard diffusion-pumped evaporation station. During this transfer, which took about ten minutes, the Si wafer was placed in a mask that contained 2.54×10^{-2}-cm-diam wires. The Cu/Al_2O_3 bilayer stripes were centered over these wires. The bell jar was then evacuated to below 4×10^{-6} Torr, which took roughly $\frac{1}{2}$ to 1 hour, and 2000 Å of Ge were evaporated through the mask to insulate the edges of the Cu/Al_2O_3 bilayers from the yet-to-be-deposited counterelectrodes. (Alternatively, thick, sputter-deposited Al_2O_3 or SiO_2 layers would be used in place of the Ge insulation, which we find generally superior for this purpose.) The samples were then again removed and the entire wafer was scribed into two halves. A mask with 2.54×10^{-2}-cm-wide slots was then used to deposit counterelectrodes perpendicular to the base electrodes. This process took less than 15 minutes after which the bell jar was again evacuated. 2000 Å of Pb or Pb-Bi were then evaporated on one half of the wafer to form the counterelectrode and complete the junction. The Pb-Bi was composed of 29 wt. % Bi as measured on a triple-beam balance accurate to 0.01 g. The amount of mixture obtained was enough to fill a standard thermal-evaporation boat which was preheated without evaporation prior to deposition to insure proper alloying of the Pb and Bi components. During this deposition the other half of the wafer was also placed in the bell jar in order to limit any natural-oxide growth. The same procedure used for Pb(Bi) counterelectrodes was employed in depositing a 2000 Å Cu counterelectrode on the remaining half of the wafer. The final product left us with about 15 potential junctions with an effective area of 6.45×10^{-4} cm^2 with an equal number of Cu and Pb (or Pb-Bi) counterelectrodes. A representative schematic of resulting junctions created by the method described earlier is shown in Fig. 2(a). Samples composed of multiple metal-Al_2O_3 layers were also made, using a similar layer-by-layer mechanical technique, as shown in Fig. 2(b).

Electrical measurements were made by mounting samples onto a simple copper-block "dipstick" measurement probe and leads were attached to the sample with indium solder. Measurements were made by voltage biasing the

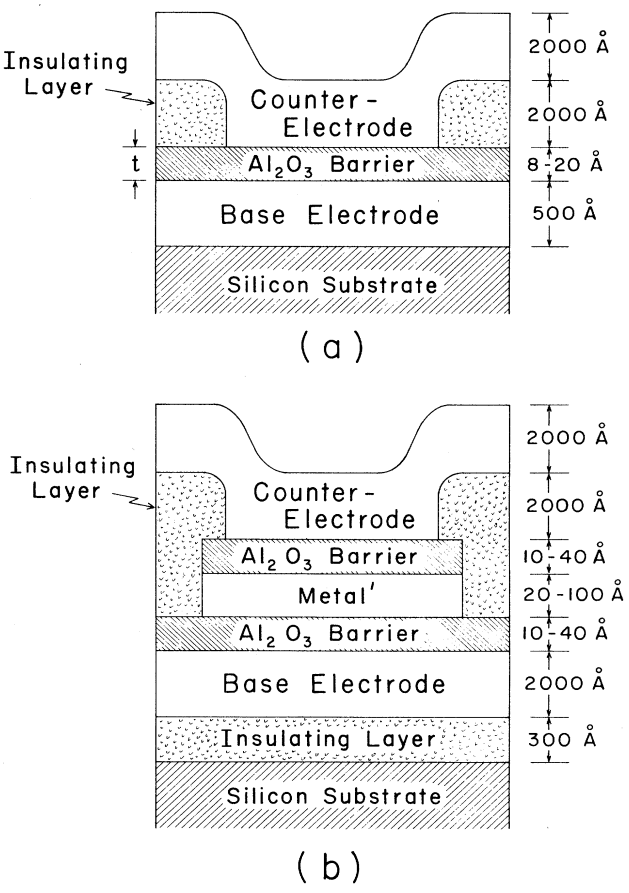

FIG. 2. Shown in (a) is a schematic of the junctions used to study the electrical properties of sputter-deposited Al_2O_3 artificial barriers. Cu/Al_2O_3 bilayers were deposited *in situ* onto room-temperature silicon substrates by the rf sputtering of a pressed Al_2O_3 target in a pure argon atmosphere. The thickness of the Al_2O_3 films varied from 8 to 20 Å. Shown in (b) is a schematic of the junctions used to study the conduction properties of the thin metal layers by electron tunneling.

junctions with a source developed by us for this purpose.[35] Current versus voltage, *I-V*, measurements of the junctions were directly chart recorded at temperatures of 77, 4.2, and sometimes <1 K. Junction resistance was defined as the slope of the *I-V* curve in the (5–50)-mV bias range.

III. MATERIAL PROPERTIES

The physical and chemical properties of the aluminum oxide films are interesting in themselves and important to the understanding of the deposition process involved in and the interpretation of the tunneling results for the films. In general, one desires a chemically robust material which is less likely to react with or give up oxygen to either the base- or counter-electrode films. For these reasons alone, then, it is desirable that the barrier material be of the form of Al_2O_3.

In order to reliably establish their chemical composition, x-ray photoelectron spectroscopy (XPS) was used to analyze the films. Incorporated in the system employed for these studies was an ion mill, making it possible to analyze both the film surface and its interior. The 300-Å-thick film used for this work was deposited onto Si under the same conditions used for barriers and was analyzed to a terminal depth of 150 Å, the results of which are presented in Fig. 3. The data shown here were taken at a depth of 100 Å and typical of the spectra obtained throughout the film. Also included are Gaussian fits to the data, based on the assumption that only a single peak is present in the data.

Taking into account the peak positions, lack of any satellite peaks, and high degree of correspondence between the data and the fit, it is estimated that no less than 99% of the aluminum oxide is of the form Al_2O_3. In fact, the results presented here were indistinguishable in terms of both peak position and detailed shape from those for a pure Al_2O_3 standard. We also note that *in situ* XPS results obtained on the surface of similarly prepared aluminum-oxide films are consistent with these results.[2,36]

Electron-diffraction measurements were also made on our Al_2O_3 films. In one case, a 300 Å-thick film was deposited onto photoresist and then lifted off, showing no evidence of crystallinity. In a second set of experiments, Al_2O_3 was deposited directly onto amorphous-carbon-coated TEM grids. In this case, the films exhibited a small-grain polycrystalline structure. Our present results, then, do not definitively answer the question of the structure of the Al_2O_3 films when incorporated into junctions. Since it has been shown[2] that Al_2O_3 tends to be polycrystalline, especially when deposited at elevated temperatures, and since the deposition conditions for Al_2O_3 barriers in junctions more closely correspond to those which lead to polycrystalline material, it appears most likely that our barriers are to some degree polycrystalline.

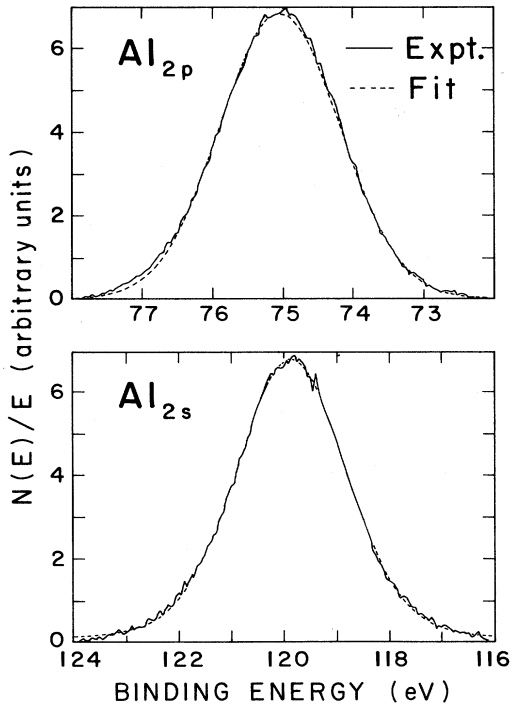

FIG. 3. X-ray photoelectron spectrum showing the Al, 2*p*, and 2*s* (top and bottom) peaks of a sputter-deposited, 300-Å-thick aluminum-oxide film taken at depth of 150 Å and representative of data obtained throughout the depth of the film. The presence of single, satellite-free peaks indicate that the Al is in a single chemical state. Analysis of the data show the film to be composed of no less than 99% Al_2O_3.

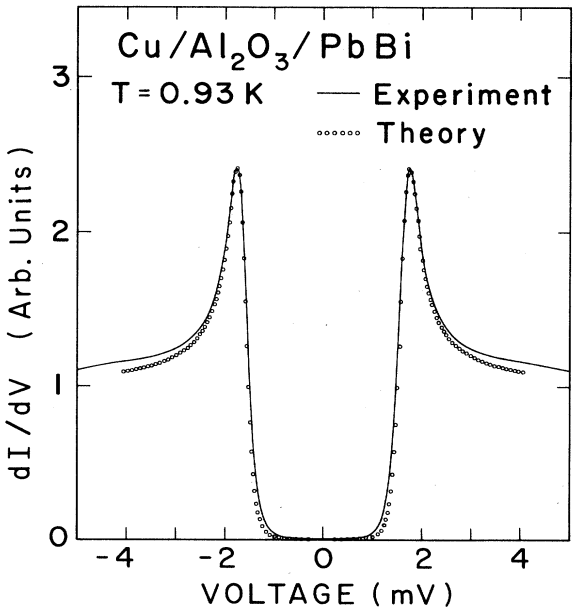

FIG. 4. Plotted here is the conductance, dI/dV, vs bias for a typical $Cu/Al_2O_3/Pb$-Bi tunnel junction with a 10-Å barrier thickness taken at 0.93 K. The amount of nontunneling, or "leakage," conductance at zero bias is less than 0.4% of the conductance above the gap.

IV. ELECTRICAL PROPERTIES

A. Single-barrier systems

One stringent test of an electron-tunnel barrier is the amount of nontunneling conduction present below the sum gap when one or both of the junction electrodes are superconducting. Also important is the presence of a full superconducting gap and associated sharp conductance rise at the gap voltage—with the absence of overshoot—indicating the presence of a clean superconductor-barrier interface and the absence of proximity effects. Demonstrating these characteristics are the results presented in Fig. 4 for a $Cu/Al_2O_3/Pb$-Bi tunnel junction measured at 0.93 K. The ac modulation used during the measurement was 0.15 mV peak-to-peak. As can be seen, clear, sharp Pb-Bi gap structure is present. To further illustrate this, a theoretical BCS fit[37] is also shown, using a gap value of 1.65 meV. The amount of nontunneling or "leakage" conduction, the conduction at zero bias compared to the normal-state value (theoretically infinitesimal at this temperature), was less than 0.4%. Absent in the data is any structure which would indicate the presence of proximity-effect tunneling which, if present, would be manifest as an overshoot in the conductance at the gap.

The deviations from the BCS fit at biases above 3 mV are associated with the Pb-Bi phonons, as expected for a strong-coupling superconductor. This structure is more clearly revealed in Fig. 5 where we show the second-harmonic signal, $-d^2I/dV^2$, versus applied bias for the same junction. Evident are the well-defined transverse and longitudinal Pb-Bi acoustic phonon peaks. The strength of the observed phonon scattering, comparable in magnitude to earlier native-oxide-barrier results,[38] demonstrates the absence of significant scattering of tunneling electrons within the barrier itself, which would tend to attenuate the peaks.[22]

At low bias, then, our artificial Al_2O_3 barriers appear to be functionally and electrically equivalent to native-oxide barriers. However, the spectroscopy of junctions at high biases does reveal an interesting difference in the two. Native aluminum oxide junctions typically show a strong asymmetry in conduction at high bias, which is strongest for those exhibiting large barrier heights.[39] Phenomenologically, this asymmetry is closely related to the strength of additional conductance structure in the 50–500 mV bias range. This structure and associated barrier asymmetry, attributed to chemical species on the surface of the tunnel barrier, is typically more clearly resolved in second-derivative measurements. In the context where junctions are deliberately exposed to chemical species, the study of such structure is normally referred to as inelastic electron-tunneling spectroscopy (IETS).[40–42]

By contrast, our and other sputter-deposited oxide barriers show none of this structure and—as typified by the data of Fig. 6—exhibit highly symmetric conductance curves. This symmetry is observed in all of our junctions with sputtered Al_2O_3 barriers, regardless of base- or counter-electrode material. One measure of the degree of symmetry is to compare the two polarity biases at which the conductance doubles its minimum value, so-called "doubling" voltages. We typically observe less than a 5% difference in the doubling voltage for a given junction, whereas for native-oxide barriers the asymmetry can be as large as 100% or more.[39]

Note that the signal-to-noise ratio of the data shown in Fig. 5 is roughly 25 and that the phonon structure represents about a 5% conductance modulation. Considering that the magnitude of typical IETS structure is roughly 10% of that associated with phonons, then such structure should be easily resolved by our spectrometer if present. In order to convince ourselves that it was indeed possible to resolve IETS structure with our setup, we performed measurements on native aluminum oxide samples

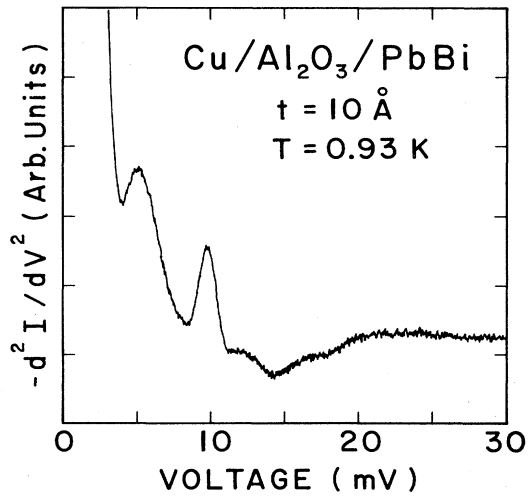

FIG. 5. Shown here is the second-harmonic signal (proportional to d^2I/dV^2), vs V, for the junction shown in the previous figure, emphasizing the Pb-Bi phonon structure. The presence of clear, strong (transverse and longitudinal acoustic) phonon peaks is representative of clean barrier tunneling.

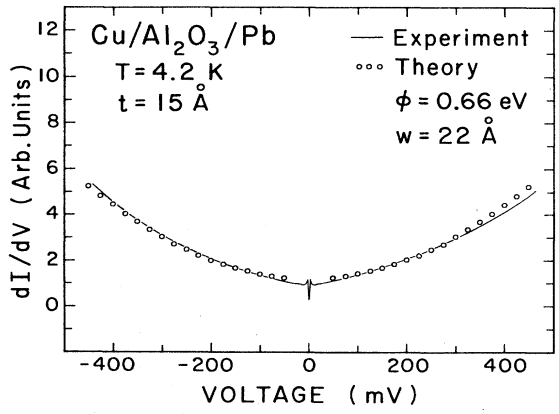

FIG. 6. Conductance, dI/dV, vs applied bias for a representative $Cu/Al_2O_3/Pb$ junction at 4.2 K. Noteworthy is the symmetry and featurelessness of the data on this scale.

fabricated in our laboratory. These revealed the expected strong, rich IET spectra and asymmetrical behavior in the conductance with bias.

The high degree of symmetry and corresponding absence of IETS structure observed for sputter-deposited oxide barriers may be caused by (1) the absence of those foreign chemical species at the barrier surface present for native oxides and/or (2) a rough oxide surface for artificial barriers, which can reportedly attenuate IETS structure.[43] Although it is also possible that junction "leakage" at high bias could tend to smooth fine structure and produce more symmetric conductance curves,[44] careful fits of several sets of data to the Brinkman theory[39]—a typical example of which is shown in Fig. 6—suggest that this is not a problem. As can be seen, the theory is in good accord with experiment—deviations presumably representative of small, intrinsic barrier asymmetry. This suggests the absence of anomalous high-bias conduction via nontunneling channels.

We finally note that the strength of IETS structure, or at least barrier asymmetry, has been shown to be material dependent, as shown by studies of rare-earth native-oxide barriers.[45] It has also been shown to be preparation dependent, as described for the case of artificial Al_2O_3 barriers themselves since the original work on *e*-beamed barriers deposited onto 77 K substrates[26] did show asymmetries similar to native Al_2O_3 barriers which were in turn dependent on electrode material. However, recent work with various artificial barriers deposited at elevated substrate temperatures always produced symmetric conductance curves, as well diminished IETS structure—independent of whether the barrier material was *e*-beam or sputter deposited.[2,36] Therefore, the lack of asymmetry and IETS structure appears to be associated primarily with the sputter-deposition process itself, perhaps in conjunction with elevated substrate temperatures.

An intrinsic advantage in studies of artificial versus natural-oxide barriers is that barrier thickness is a directly accessible parameter, in so far as the deposited thickness can be determined. Thus, although the absolute accuracy of the barrier thickness is to some degree subject to systematic error, the ratio of thickness from one run to another—the proportional barrier thickness—is accurately known.

One junction parameter we have examined as a function of deposited barrier thickness is the amount of leakage conduction present at zero bias when a superconducting counterelectrode is employed. In Fig. 7 we present a study of four $Cu/Al_2O_3/Pb$-(Bi) junctions. Evident here, and representative of our results in general, is the distinctly lower leakage in junctions with Al_2O_3 thicknesses greater than 8 Å. These results imply the existence of a relatively well-defined minimum thickness for our barriers which is in the vicinity of 8 Å. With other techniques, it has been shown possible to reduce this cutoff to only 3 Å.[2]

What is the origin of this cutoff thickness for our barrier films? Some insight can be gained by considering the results of Fig. 8, which shows junction yield—as a percent of the total number, N, of samples fabricated—as a function of barrier thickness. The error is assumed to

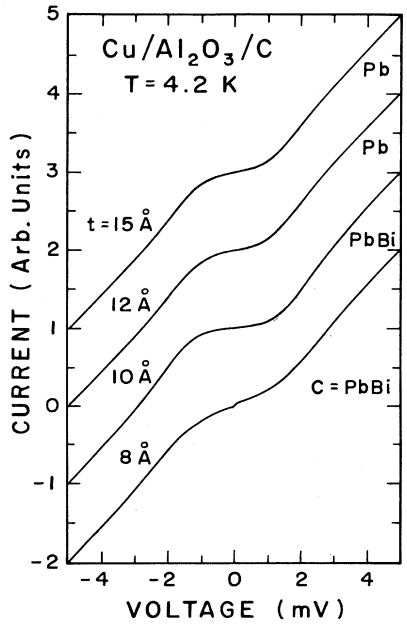

FIG. 7. A series of *I-V* characteristics taken at 4.2 K is shown for junctions with Pb(Bi) counterelectrodes, with deposited barrier thickness running from 15 to 8 Å, (top to bottom). The data have been offset for clarity and normalized such that the normal-state resistance is represented by a 45° line. For barrier thicknesses exceeding 8 Å the leakage conduction is low (typically on the order of 1%). 8 Å barrier thickness, the point at which leakage typically becomes noticeably higher, appears to represent the lower limit for obtaining low-leakage junctions.

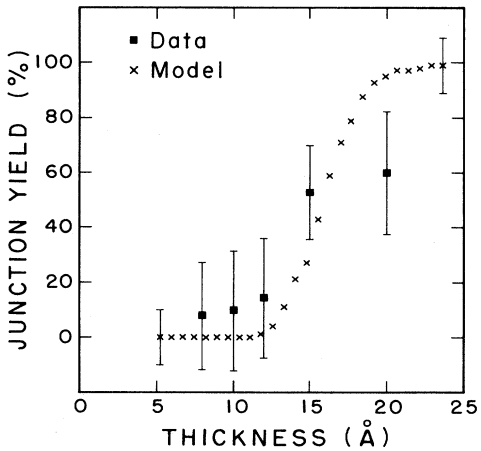

FIG. 8. Junction yield (or, percent of samples exhibiting tunneling) is plotted vs deposited barrier thickness, t. There is a systematic improvement in the probability of obtaining a good junction with increasing t. The data have been modeled assuming the random covering of a surface with a finite number of spheres having zero mobility and a sticking coefficient of unity. A successful junction is created if the surface gets fully covered. The results of calculations with this model are also indicated on the plot. The good accord between this simple model and our experimental results suggests that barrier growth occurs in a statistical fashion.

scale like $N^{1/2}/N$. Here, the criterion used to distinguish successful from failed junctions was the presence of any characteristic normally associated with tunneling. These include positive curvature of conductance with bias (as opposed to electrical shorts which exhibit negative curvature), increasing resistance with decreasing temperature, and—in the case of superconducting counterelectrodes—the presence of a superconducting gap. Although these can be rather lax criteria, they effectively serve to characterize the basic systematics of junction "success" rate as a function of barrier thickness.

Returning to Fig. 8 we can see that, as expected, junctions with thicker barriers indeed have a higher success rate, and, furthermore, that plotting the data in this way reveals a well-defined turn-on of success rate in the (12–15)-Å barrier-thickness range. We note further that if we reserve the definition "high quality" for junctions whose barriers have heights in excess of 0.95 eV and zero-bias leakage on the order of 1%, then the same systematics in the data are reproduced as a function of thickness; in particular, an increase in the success rate from 3% at 10 Å to 10% at 20 Å. This result is reminiscent of what is commonly observed for conduction thresholds in percolative systems and has been modeled as such. To do this we took the Al_2O_3 molecules to be spheres incident on and randomly filling vertical cells forming a square, two-dimensional lattice. Successful barrier formation was defined as the point at which each cell was filled with at least one sphere; that is, the point at which the surface was completely covered. The ratio between the actual thickness of the deposited films and the number of layers was taken to be 5.3 Å/layer, 5.3 Å being the equivalent diameter of a sphere with its volume taken as that of the unit cell of Al_2O_3.[46] A layer in the model was defined as the number of spheres placed in the grid divided by the number of slots in the grid. A 100×100 grid was used and the calculation was repeated 100 times for each layer.

We see that the trend of the calculation is in good accord with our observations even with this simple model, and reproduces the conductance turn-on very close to the point at which it is experimentally observed. This implies that the growth mechanism of these barrier films is a random covering of the surface of the (Cu) base electrode with Al_2O_3 molecules. Although the model actually predicts that more junctions should result than were actually observed at a thickness greater than 15 Å, this may be due to the assumption of a nonzero surface mobility for the Al_2O_3 molecules and/or a greater affinity of Al_2O_3 for Cu as compared to itself, either of which would tend to increase the success rate at a given thickness. These results also suggest that native-oxide formation does not significantly aid in successful barrier formation here, as this would lead to a much less critical behavior on the junction yield as a function of deposited thickness.

We have also examined the systematics of the calculated effective barrier heights and widths observed for our junctions using the Simmons model[47] as modified by Brinkman, *et al.*[39] The two input parameters to the theory are the doubling voltage—the voltage at which the conductance is twice its zero-bias value—and the product of junction resistance and area, RA. In a number of cases, as with the data shown in Fig. 6, we also fit the entire I or dI/dV versus V curves (as opposed to just the doubling voltage) to verify that there were no significant differences in the resultant implied values of barrier height and width. Defining good junctions as those with barrier heights in excess of 0.95 eV and leakage below 1%, effective barrier height is seen to increase from 1 eV at $t=10$ Å to 2.3 eV at $t=20$ Å. For the remaining class of junctions, we find a general decrease of barrier height with increasing effective barrier width which resembles the results for native aluminum oxide where these parameters have been deduced in a similar fashion.[29] The results of these calculations for junctions made over the past few years are listed in Table I.

In light of these results, it is instructive to compare the actual deposited barrier thickness, t, to the effective barrier widths, w, calculated as discussed earlier. This is shown in Fig. 9. Note that points for good quality barriers, (■), tend to lie close to this line while those with inferior characteristics (□) tend to lie off the line. Therefore, although barriers are certainly more complex than the simple rectangular-barrier model would imply, the data show that for high quality barriers there is a tendency for the effective and actual barrier thicknesses to be comparable—suggesting that these barriers are rectangular-like in nature notwithstanding the reduction of barrier height from its ideal value.

One essential criterion for tunneling is an exponential increase of junction resistance with increasing barrier thickness. To demonstrate this in our data, we present in Fig. 10 the product of junction resistance and area, RA, versus deposited barrier thickness, t, for a number of junctions with both Al_2O_3 (solid points) and, for comparison, MgO data from other workers (open symbols). These include MgO barriers in the 5–10 Å range,[1] (○) and MgO (Ref. 3) (△), and MgO-CaO (Ref. 2) (□) barriers thicker than 10 Å. It is clear that, for a given set of junctions, the expected overall exponential rise in resistance with barrier thickness is obtained. It can also be seen that for the Al_2O_3 data junctions with Pb and then Pb-Bi counterelectrodes tend to have larger resistances than those with Cu counterelectrodes at a given barrier thicknesses, suggesting a lesser degree of reactivity for these materials.

More globally speaking, there are clearly two types of behavior present. For our Al_2O_3 and for the thinner MgO-barrier data, there is a rapid, exponential rise in resistance for barrier thicknesses up to 20 Å, whereas for the MgO (CaO) data above 10 Å there is a much more gradual—yet still exponential—growth in resistance.

From these data an effective barrier height can be immediately deduced by adopting a simple rectangular-barrier model and noting that barrier width is simply the deposited barrier thickness. In the limit where bias voltage $V\rightarrow0$, the product of resistance and area is given by[48]

$$RA=3.17\times10^{-11}(t/\phi^{1/2})\exp[2t(2m_e e\phi)^{1/2}/\hbar]$$

$$=3.17\times10^{-11}(t/\phi^{1/2})\exp(1.025t\phi^{1/2})\,, \qquad (1)$$

to $O(V)$,[49] where t is in units of Å, ϕ is in units of eV, and RA is in units of $\Omega\,cm^2$. Alternatively, an effective decay length can be defined, by assuming a simple exponential decay of the tunneling wave function, as

$$RA = C\exp(t/\alpha)\ . \tag{2}$$

Fits to Eq. (1) were made with ϕ as the only adjustable parameter and with Eq. (2) with both C and α as adjustable parameters. The results of these fits are shown in the figure where we note that the appropriate value of C for our data (solid points) was $2.12\times10^{-9}\ \Omega\,cm^2$. For the first (○) and second (△,□) MgO (CaO) data sets C took on values of 1.69×10^{-11} and $4.87\times10^{-6}\Omega\,cm^2$, respectively. We note that if we take $\alpha^{-1}=1.025\phi^{1/2}$ in Eq. (2), then reported barrier-height values[1,2] are seen to be consistent with our deduced values of the decay length.

We see that for our data (solid points) and the MgO data at small thickness (○), both Eqs. (1) and (2) are in good accord with the data, producing values of ϕ in the vicinity of 1–2 eV and α of roughly 1 Å. We also note that the average value of ϕ for our data of 1.65 eV falls in the range obtained by the calculation with the Brinkman *et al.* theory of 1–2.3 eV for individual junctions. Finally we see that for MgO (CaO) barriers thicker than 10 Å, there is a lower slope in RA. For these data only Eq. (2) produces an adequate fit to the data, giving a decay length of 7 Å.

In considering these two types of behavior, it must be kept in mind that the NbN base electrode is assumed to contribute to the MgO barrier—principally by the formation of native oxides which are believed to plug pinholes in the artificial barrier.[3] One view of the ob-

TABLE I. Listed below are the measured and calculated parameters for our junctions with sputter-deposited Al_2O_3 barriers in the form $Cu/Al_2O_3/C$. Note that the last two junctions listed in the table are $Cu/Al_2O_3/Cu$ trilayer samples, prepared entirely *in situ*.

Sample	Deposited barrier thickness t (Å)	Resistance × Area RA (Ωcm^2)	Barrier height ϕ (eV)	Barrier width w (Å)	Counter electrode (C)
1	20.0	2.11×10^{4}	2.260	20.3	Pb
2	20.0	2.32×10^{3}	0.050	112.0	Pb
3	20.0	2.58×10^{4}	1.660	23.8	Pb
4	20.0	2.42×10^{2}	0.570	33.3	Pb
5	20.0	2.36×10^{2}	0.564	34.4	Pb
6	20.0	1.35×10^{2}	0.445	36.7	Pb
7	20.0	1.55×10^{3}	1.950	20.6	Pb
8	20.0	1.10×10^{2}	0.936	26.5	Pb
9	20.0	2.41×10^{1}	0.580	33.1	Cu
10	20.0	2.23×10^{0}	1.100	20.4	Cu
11	20.0	6.14×10^{1}	0.530	32.7	Cu
12	20.0	1.62×10^{2}	0.367	40.4	Cu
13	15.0	1.01×10^{1}	0.250	43.0	Pb
14	15.0	5.68×10^{0}	0.614	27.8	Pb
15	15.0	1.72×10^{1}	0.171	52.3	Pb
16	15.0	5.48×10^{0}	0.287	39.3	Pb
17	15.0	1.26×10^{-1}	0.630	23.0	Pb
18	15.0	9.68×10^{-3}	0.470	22.8	Pb
19	15.0	7.68×10^{-2}	1.050	18.5	Pb
20	15.0	1.16×10^{-2}	0.790	18.4	Cu
21	15.0	2.23×10^{-2}	0.950	17.5	Cu
22	15.0	4.61×10^{-3}	0.750	18.5	Cu
23	15.0	3.01×10^{-3}	0.790	17.6	Cu
24	15.0	2.83×10^{-3}	0.776	17.8	Cu
25	15.0	4.54×10^{-3}	0.610	19.4	Cu
26	15.0	7.03×10^{-4}	0.660	16.7	Cu
27	15.0	5.19×10^{-4}	0.950	13.9	Cu
28	15.0	9.22×10^{-3}	0.860	17.5	Cu
29	15.0	1.19×10^{1}	0.599	29.9	Cu
30	12.0	1.03×10^{0}	0.580	26.5	Pb
31	12.0	2.90×10^{-1}	1.380	16.8	Pb
32	12.0	8.90×10^{-4}	0.580	17.9	Cu
33	10.0	5.37×10^{-3}	1.050	15.5	Pb-Bi
34	10.0	7.29×10^{-3}	0.870	17.1	Pb-Bi
35	20.0	1.11×10^{-4}	0.058	58.8	Cu
36	20.0	1.77×10^{-2}	1.260	19.3	Cu

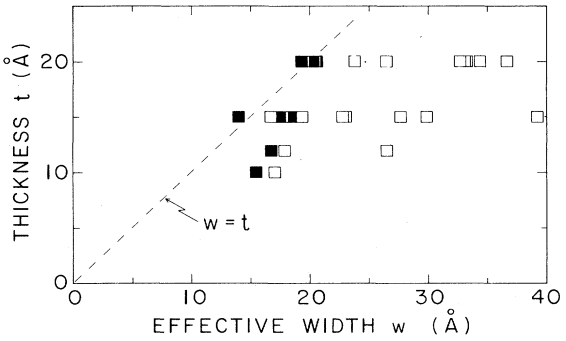

FIG. 9. Plotted is the deposited thickness, t, vs the calculated effective width, w, of sputter-deposited Al_2O_3 barriers. Note for a set of high quality barriers, those having barrier heights in excess of 0.95 eV and leakage $<1\%$ (■), there exists a close correspondence between w and t.

served results, then, is that when the deposited MgO barrier is very thin its conductance dominates over that of the native NbN oxide, and thus variations in MgO thickness are directly reflected in the growth of resistance. At higher barrier thicknesses, however, as the resistance of the artificial barrier grows larger, resistance changes reflect the more complex combination of native and artificial elements of the barrier, the lower slope reflecting

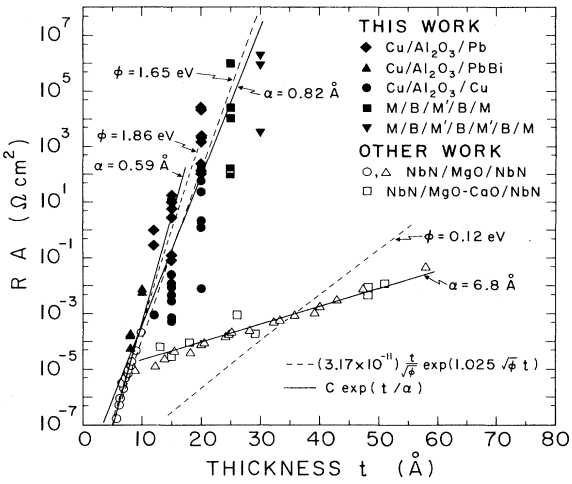

FIG. 10. Shown is the product of junction resistance and area, RA, plotted on a log scale vs the deposited Al_2O_3 thickness, t. The data (solid points) here represent both single- and multiple-barrier junctions, as indicated in the figure. Evident is the exponential rise of resistance with increasing thickness expected for tunneling. The effect of counter-electrode material is also evident and manifest by the presence of two distinct populations of data lying near the upper [for Pb(Bi)] and lower (for Cu) portions of the plot. Also shown are data for MgO (○,△) and MgO-CaO (□) barriers, Refs. 1, 3, and 2, respectively. The dashed lines are fits to theory, giving the average barrier height, ϕ, and the solid lines are fits to a simple exponential variation used to define an effective decay length, α. Note that the predicted resistance-vs-thickness dependence is in good accord with our Al_2O_3 data.

the contribution of the inferior native oxides. The complex nature of the barrier (and very low effective barrier height) in this regime may also explain the failure of Eq. (1), the complete tunneling theory result for a simple rectangular barrier, to fit these data.

We reemphasize here that in our studies, Cu base electrodes were employed with the assumption that oxidation of the Cu which took place (through the Al_2O_3 barrier) would not be effective in assisting in barrier formation and thus would allow for a study of the properties of the Al_2O_3 alone. In fact, we also have made samples of the form $Cu/Al_2O_3/Cu$ prepared *in situ,* measurements of which confirmed that even when samples were never exposed to oxygen no degradation of intrinsic barrier properties took place. Thus we see that overall, as has been seen in other experiments with inert base electrodes,[26,29] the intrinsic properties of deposited-oxide barriers can be excellent.

Returning to Fig. 10, then, we see that the results for our Al_2O_3 barriers continue along the trend set by the MgO data at small thicknesses. This is consistent with the idea that this trend reflects the rise in resistance due to Al_2O_3 barrier itself. It is consistent also with the assumption that since Cu is used as the base electrode, its oxide does not assist in barrier formation. Also, as noted before, our statistical model of the barrier, in conjunction with measured junction success rates, indicates that the barrier completely covers the base electrode for thicknesses greater than 8 Å. Therefore, at least up to the thicknesses reported, the effective barrier parameters indicated are assumed to reflect the intrinsic properties of the artificial Al_2O_3 barrier material. In fact, attempts to observe any crossover behavior in junction resistance for thicker Al_2O_3 barriers failed due to the impracticably large resistances encountered for junctions thicker than 30 Å, suggesting a continued trend in RA versus thickness beyond the data as shown.

One additional property, important in establishing tunneling properties of our Al_2O_3 films, is the change in junction resistance as a function of temperature. According to theory[47] one can estimate, using reasonable values for the effective barrier height and thicknesses, that the increase in junction resistance for cooling from 77 to 4.2 K should be less than or in the vicinity of 5% if conduction is by electron tunneling alone. We have carefully examined the resistance of our junctions at these two temperatures and found that for lower resistance ($<100\ \Omega$) junctions the change in resistance is indeed consistent with this expectation. For higher resistance junctions we also see such results when junction base-electrode–barrier edges are insulated with (see Fig. 2) a low-conductance material such as Al_2O_3 or SiO_2 as opposed, for example, to Ge which is seen to contribute to the temperature dependence of very high resistance junctions.

B. Multiple-barrier systems

We have also employed our artificial barriers to study multilayer tunnel systems. Present work has focused on systems of the form $E/Al_2O_3/M'/Al_2O_3/C$, where E and C denote base electrode and counterelectrode, respective-

ly, with M' layers normal-metal films less than 100 Å in thickness. These systems are schematically depicted in Fig. 2(b) (lower figure).

To assure ourselves that the barriers performed satisfactorily in these systems, a similar study of thickness-dependent tunneling parameters was undertaken. Results for junction resistance are shown in Fig. 10 for systems with 2 or 3 barriers, for which the measured resistance was assumed to be the series combination of the barriers. The tunnel systems denoted in Fig. 10 as $M/B/M'/B/M$ and $M/B/M'/B/M'/B/M$ were Cu/Al_2O_3(25 Å)/Ag(75 Å)/Al_2O_3(25 Å)/Ag and Ag/Al_2O_3(30 Å)/Ag(75 Å)/Al_2O_3(30 Å)/Ag(75 Å)/Al_2O_3(30 Å)/Ag, respectively. These results, consistent with the trends established by the single-barrier results, indicate that the important intrinsic properties of the barriers themselves are preserved when they are incorporated in multiple-junction systems.

The detailed conductance properties of these multilayer junctions, however, are dramatically different from single-barrier systems in two significant ways and has to do with the presence of the M' layer. One is immediately obvious in Fig. 11, in which we show the conductance, dI/dV, versus applied bias measured at both 4.2 and 77 K for a junction comprising a thin (75 Å) film of Ag sandwiched between two barriers as: $Cu/Al_2O_3/Ag/Al_2O_3/Ag$ as shown in the inset of Fig. 11. The most prominent feature, a decrease of conductance in the vicinity of zero bias, has been previously observed on this energy scale by Giaever and Zeller.[50] They performed tunneling experiments on Sn droplets sandwiched by natural oxide between electrodes in an overall geometry much like ours. They identified this "zero-bias" anomaly, or Coulomb blockade, as originating from the charging of the Sn particles by tunneling electrons. Based on these results, our Ag films were studied by transmission electron microscopy and were, indeed, found to be comprised of small particles with diameters of roughly the thickness of the deposited film.

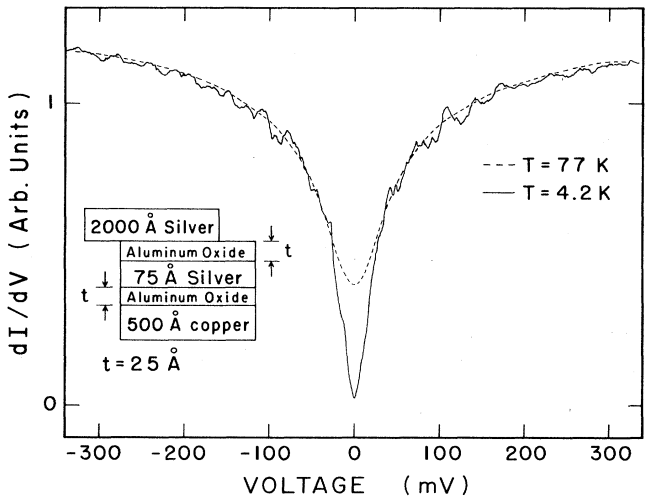

FIG. 11. Conductance data for a double-barrier tunnel systems at 77 and 4.2 K. Similar strong conductance depressions zero bias was previously observed by Gaiever and Zeller (Ref. 50). A new observation is the series of peaks in conductance seen on top of the stronger zero-bias anomaly. These have been identified as a manifestation of higher-order, single-electron charging effects (Refs. 6 and 7). This structure disappears at higher temperatures.

More careful inspection of the conductance curve at 4.2 K reveals further structure on top of the zero-bias dip in the form of a periodic series of conductance peaks reported by us,[6,7] Likharev *et al.*,[51] and most recently by van Bentum *et al.*[52] These peaks have been identified with higher-order charging effects involving the incremental charging of the Ag particles by 0,1,2,3,. . . electrons—so-called single-electron charging effects. These effects have been discussed theoretically by Averin and Likharev,[53] and Mullen and Ben-Jacob.[54] A discussion of our experimental work on these systems will be the topic of a more comprehensive regular article.

These results demonstrate both an exciting example of new physics made observable with multiple-barrier systems, and the potential for new experimental systems now possible with the availability of artificial barriers.

V. CONCLUSIONS

We have demonstrated the ability to employ rf-sputtered Al_2O_3 films as a high quality artificial tunnel barriers. The films are composed of $>99\%$ Al_2O_3 as determined by XPS. Tunneling studies of junctions incorporating these barriers reveal full, clean superconducting-gap structure, low subgap conduction, and sharp, distinct phonon spectral peaks, an exponential growth of resistance with barrier thickness, and an appropriate (less than 5%) decrease in tunnel resistance when junctions are cooled from 77 to 4.2 K—all of which are evidence for tunneling as the principle conduction channel through the barriers.

The largest individual barrier height we obtained by fitting conductance data out to high bias was 2.3 eV and we observed a systematic increase in the barrier heights of individual high quality (low leakage) junctions of from 1 to 2.3 eV for barrier thicknesses in the range of 10–20 Å. The average barrier height obtained from the exponential growth of junction resistance with deposited barrier thickness was 1.65 eV with a corresponding decay length of 0.82 Å. A study of junction yield as a function of Al_2O_3 thickness reveals a well-defined increase in the vicinity of 12–15 Å consistent with a statistical covering of the base electrode with Al_2O_3 molecules.

The universal adaptability of these barriers has been further demonstrated by the successful creation of $M/B/M'/B/M$ multilayer tunnel systems wherein the properties of an electrically isolated M' layer of metal droplets were studied—confirming the participation of single-electron charging effects in these systems and allowing, for the first time, an observation of the so-called Coulomb staircase expected for tunneling in ultralow-capacitance systems.

ACKNOWLEDGMENTS

The authors wish to thank M. R. Beasley, C. A. Gaffney, M. Gurvitch, J. M. Rowell, J. Talvacchio, and W. J. Tomasch, for valuable discussions, R. A. Carretta for his XPS results and A. Pelton for scanning transmission electron microscopy (STEM) studies. This work was supported by the National Science Foundation by Grant Nos. NSF ECS 85-06823 and NSF DMR 86-10375.

[1]A. Shoji, M. Aoyagi, S. Kosaka, F. Shinoki, and H. Hayakawa, Appl. Phys. Lett. **46**, 1098 (1985); A. Shoji, M. Aoyagi, S. Kosaka, and F. Shinoki, IEEE Trans. Mag. **MAG-23**, 1464 (1987).

[2]A. I. Braginski, J. R. Gavaler, M. A. Janocko, and J. Talvacchio, in *SQUID '85, West Berlin, 1985,* edited by H. D. Hahlbohm and H. Lübbig (de Gruyter, New York, 1985), p. 591; J. Talvacchio and A. I. Braginski, IEEE Trans. Mag. **MAG-23**, 859 (1987); J. Talvacchio, A. I. Braginski, M. A. Janocko, and J. R. Gavaler, Bull. Am. Phys. Soc. **31**, 438 (1986); J. Talvacchio, S. Sinharoy, and A. I. Braginski, J. Appl. Phys. **62**, 611 (1987); J. Talvacchio, J. R. Gavaler, and A. I. Braginski, in *Metallic Multilayers and Epitaxy,* edited by M. Hong, S. A. Wolf, and D. C. Gubser (The Metallurgical Society, Warrendale, PA, 1988), pp. 109–134.

[3]H. G. LeDuc, J. A. Stern, S. Thakoor, and S. K. Khanna, IEEE Trans. Mag. **MAG-23**, 863 (1987); H. G. LeDuc, S. Thakoor, and S. K. Khanna, Bull. Am. Phys. Soc. **31**, 438 (1986); S. Thakoor, H. G. LeDuc, J. A. Stern, A. P. Thakoor, and S. K. Kahanna, J. Vac. Sci. Technol. A **5**, 1721 (1987).

[4]T. Yamashita, K. Hasmaski, and T. Komata, Adv. Cryog. Eng. Mater. **32**, 617 (1986).

[5]E. K. Track, L.-J. Lin, G.-J. Cui, and D. E. Prober, Adv. Cryog. Eng. Mater. **32**, 635 (1986).

[6]J. B. Barner and S. T. Ruggiero, Phys. Rev. Lett. **59**, 807 (1987).

[7]S. T. Ruggiero and J. B. Barner, Phys. Rev. B **36**, 8870 (1987).

[8]D. F. Moore, R. B. Zubeck, J. M. Rowell, and M. R. Beasley, Phys. Rev. B **20**, 2721 (1979).

[9]D. A. Rudman and M. R. Beasley, Appl. Phys. Lett. **36**, 1010 (1980).

[10]D. A. Rudman, R. E. Howard, D. F. Moore, R. B. Zubeck, and M. R. Beasley, IEEE Trans. Mag. **MAG-15**, 582 (1979).

[11]R. Meservey, P. M. Tedrow, and J. S. Brooks, J. Appl. Phys. **53**, 1563 (1982).

[12]S. Celaschi, J. Appl. Phys. **60**, 296 (1986).

[13]S. J. Bending and M. R. Beasley, Phys. Rev. Lett. **55**, 324 (1985); S. Bending, R. Brynsvold, and M. R. Beasley, Adv. Cryog. Eng. Mater. **32**, 499 (1986).

[14]H. Kroger, C. N. Potter, and D. W. Jillie, IEEE Trans. Mag. **MAG-15**, 488 (1979); H. Kroger, IEEE Trans. Electron Devices **ED-27**, 2016 (1980).

[15]E. L. Wolf, J. Zasadzinski, J. W. Osmun, and G. B. Arnold, J. Low Temp. Phys. **40**, 19 (1980).

[16]M. Gurvitch, M. A. Washington, and H. A. Huggins, Appl. Phys. Lett. **42**, 472 (1983).

[17]M. Gurvitch, M. A. Washington, H. A. Huggins, and J. M. Rowell, IEEE Trans. Mag. **MAG-19**, 791 (1983).

[18]J. M. Rowell, M. Gurvitch, and J. Geerk, Phys. Rev. B **24**, 2278 (1981).

[19]M. Gurvitch and J. Kwo, Adv. Cryog. Eng. Mater. **30**, 509 (1983).

[20]J. Kwo, G. K. Wertheim, M. Gurvitch, and D. N. E. Buchanan, IEEE Trans. Mag. **MAG-19**, 795 (1983).

[21]S. Celaschi, R. Hammond, T. H. Geballe, and W. P. Lowe, Bull. Am. Phys. Soc. **28**, 423 (1983); S. Celaschi, T. H. Geballe, and W. Lowe, in Proceedings of the Material Research Society, 1982, Annual Meeting of the Materials Research Society, Boston, MA (unpublished), p. 241.

[22]S. T. Ruggiero, E. K. Track, D. E. Prober, G. B. Arnold, and M. J. DeWeert, Phys. Rev. B **34**, 217 (1986); S. T. Ruggiero, D. W. Face, and D. E. Prober, Bull. Am. Phys. Soc. **28**, 423 (1983); S. T. Ruggiero, D. W. Face, and D. E. Prober, IEEE Trans. Mag. **MAG-19**, 960 (1983); S. T. Ruggiero, G. B. Arnold, E. Track, and D. E. Prober, IEEE Trans. Mag. **MAG-21**, 850 (1985).

[23]C. P. Umbach, A. M. Goldman, and L. E. Toth, Appl. Phys. Lett. **40**, 81 (1982).

[24]S. Morohashi and S. Hasuo, J. Appl. Phys. **60**, 3774 (1986).

[25]See, for example, R. D. Blaugher, J. X. Przybysz, J. Talvacchio, and J. Buttyan, IEEE Trans. Mag. **MAG-23**, 673 (1987).

[26]J. S. Moodera, R. Meservey, and P. M. Tedrow, Appl. Phys. Lett. **41**, 488 (1982).

[27]M. Muck, H. J. Hedbabny, and H. Rogalla, IEEE Trans. Mag. **MAG-23**, 1493 (1987).

[28]J. B. Barner and S. T. Ruggiero, IEEE Trans. Mag. **MAG-23**, 854 (1987); J. B. Barner, S. M. Schwarzbek, and S. T. Ruggiero, Bull. Am. Phys. Soc. **31**, 437 (1986).

[29]A. F. Hebard, A. T. Fiory, S. Nakahara, and R. H. Eick, Appl. Phys. Lett. **48**, 520 (1986).

[30]H. Asano, K. Tanabe, O. Michikami, M. Igarashi, and M. R. Beasley, Jpn. J. Appl. Phys. **24**, 289 (1985).

[31]T. Yamashita, K. Hamasaki, Y. Kodaira, and T. Komata, IEEE Trans. Mag. **MAG-21**, 932 (1985).

[32]M. Tonouchi, Y. Sakaguchi, and T. Kobayashi, J. Appl. Phys. **62**, 961 (1987).

[33]US II-type sources; available from U.S., Inc., Campbell, CA.

[34]Targets available from Demetron, Inc., P.O. Box 1450, Morgan Hill, CA 95037.

[35]S. T. Ruggiero and J. B. Barner, Rev. Sci. Instrum. **58**, 2334 (1987).

[36]J. Talvacchio (private communication).

[37]Code used in fit courtesy of G. B. Arnold. An imaginary part of 1.5% was added to the superconducting gap.

[38]R. C. Dynes and J. M. Rowell, Phys. Rev. B **11**, 1884 (1975).

[39]W. F. Brinkman, R. C. Dynes, and J. M. Rowell, J. Appl. Phys. **41**, 1915 (1970). J. M. Rowell, in *Tunneling Phenomena in Solids,* edited by E. Burstein and S. Lundquist (Plenum, New York, 1969), Chap. 27.

[40]*Tunneling Spectroscopy,* edited by P. K. Hansma (Plenum, New York, 1982).

[41]*Principles of Electron Tunneling Spectroscopy,* edited by E. L. Wolf (Oxford, New York, 1985).

[42]*Inelastic Electron Tunneling Spectroscopy,* edited by T. Wolfram (Springer-Verlag, New York, 1978).

[43]W. Plesiewicz and J. G. Adler, Phys. Rev. B **34**, 4583 (1986),

and references contained therein.
[44]R. C. Jaklevic (private communication).
[45]G. A. Gaffney and W. J. Tomasch (unpublished); G. A. Gaffney, Ph.D. thesis, University of Notre Dame, 1987.
[46]R. W. G. Wychoff, *Crystal Structures* (Interscience, New York, 1964), Vol. 2. Note that there are two Al_2O_3 molecules per unit cell.
[47]J. G. Simmons, J. Appl. Phys. **34**, 238 (1963); **35**, 2655 (1964); **34**, 1793 (1963).
[48]J. G. Simmons, *Tunneling Phenomena in Solids,* edited by E. Burstein and S. Lundquist (Plenum, New York, 1969), p. 135.
[49]In the Simmon's and Brinkman *et al.* theory (Refs. 39, 47, and 48), this relation is carried to order V^2, requiring high-bias conduction measurements to deduce the effective barrier height and width (for a given junction) in conjunction with a given value of $R\,A$ for an individual junction.
[50]I. Giaever and H. R. Zeller, Phys. Rev. Lett. **20**, 1504 (1968); H. R. Zeller and I. Giaever, Phys. Rev. **181**, 789 (1969).
[51]L. S. Kuz'min and K. K. Likharev, Pis'ma Zh. Eksp. Teor. Fiz. **45**, 389 (1987) [JETP Lett. **45**, 495 (1987)].
[52]P. J. M. van Bentum, R. T. M. Smokers, and H. van Kempen, Phys. Rev. Lett. **60**, 2543 (1988).
[53]D. V. Averin and K. K. Likharev, J. Low Temp. Phys. **62**, 345 (1986); see also K. K. Likharev, IBM J. Res. Develop. **32**, 144 (1988), and references therein.
[54]K. Mullen, E. Ben-Jacob, R. C. Jaklevic, and Z. Schuss, Phys. Rev. B **37**, 98 (1988).